Int. J. Heat Mass Transfer. Vol. 31, No. 11, pp. 2285–2290, 1988
Printed in Great Britain

0017-9310/88 $3.00+0.00
Pergamon Press plc

Convective instability of a fluid layer confined in a vertical annulus heated from below

JOO SIK YOO,† MOON-UHN KIM‡ and DO H. CHOI†

Departments of †Mechanical Engineering and ‡Applied Mathematics,
Korea Advanced Institute of Science and Technology, P.O. Box 150, Cheongryang, Seoul, Korea

(*Received* 10 *February* 1988 *and in final form* 11 *April* 1988)

Abstract—The onset of natural convection in a fluid layer completely confined in a vertical annulus heated from below is investigated on the basis of linear stability theory. The critical Rayleigh numbers and the preferred cell patterns are determined as functions of the mean radius and the gap width for a given layer depth. The results are in good agreement with the experimental observations of Stork and Müller.

1. INTRODUCTION

MUCH ATTENTION has been paid to the onset of natural convection in a completely confined fluid heated from below to investigate the effects of the bounding walls. Some investigators [1, 2] have obtained analytic solutions through separation of variables by allowing slip on either lateral walls or the top and bottom surfaces. The problem with the no-slip condition on all the boundaries has been considered by many other investigators [3–8]. The onset of convection in a rectangular box of fluid heated from below has been considered by Davis [3] and by Catton [4, 5]; it is predicted that, at the onset, finite rolls (cells with two non-zero velocity components dependent on all three spatial variables) with axes parallel to the shorter side of the box appear. The onset of convection in a cylindrical fluid layer was investigated by Charlson and Sani [6, 7] and, more recently, by Buell and Catton [8]. Stork and Müller experimentally studied the onset of convection in rectangular boxes [9], cylinders and annuli [10]. Ozoe *et al.* [11] have also treated the convection problem, both experimentally and computationally, for the vertical annulus of a fluid at Rayleigh numbers far above critical. They assumed that the roll possesses a nearly square cross-section at the mean radius within the gap, which is valid for moderately small values of gap width to depth ratio (see Section 4).

This study is concerned with the onset of convection in an annulus of fluid bounded above and below by perfectly conducting plane surfaces, and laterally by two concentric vertical cylinders either perfectly conducting or perfectly insulating. All the bounding surfaces are rigid. The equations describing the dynamics of infinitesimal disturbances into an initially quiescent fluid layer heated from below are approximately solved by using the Galerkin method. Special attention is paid to determining the preferred cell patterns for various combinations of the mean radius and gap size.

2. FORMULATION OF THE PROBLEM

Initially a quiescent quasi-incompressible Boussinesq fluid fills an annular region as shown in Fig. 1. The top and bottom surfaces are assumed to be perfectly conducting and maintained at constant temperatures T_1 and T_0 ($T_0 > T_1$), respectively. The lateral walls are either perfectly conducting or perfectly insulating. In the initial state, a linear temperature profile is established in the fluid in the vertical direction. Since, in this particular problem, instability sets in via a time-independent marginal state [6], terms with time derivative can be dropped in the linearized equations governing small disturbances. In cylindrical coordinates, the linear non-dimensional equations governing infinitesimal disturbances are

$$\frac{1}{r}\frac{\partial}{\partial r}(ru_r)+\frac{1}{r}\frac{\partial u_\phi}{\partial \phi}+\frac{\partial u_z}{\partial z}=0 \tag{1}$$

$$\nabla^2\mathbf{u}+Ra\,\theta\mathbf{e}_z=\frac{1}{Pr}\nabla p \tag{2}$$

$$\nabla^2\theta+u_z=0 \tag{3}$$

where the following nondimensionalization is used:

$$(r,z)=\left(\frac{r_*}{H},\frac{z_*}{H}\right),\quad \mathbf{u}=\frac{H}{\kappa}\mathbf{u}_*$$

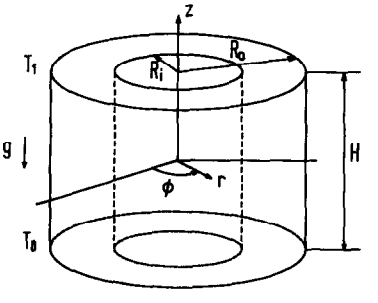

FIG. 1. Schematic of the physical system.

NOMENCLATURE

$A_{n,k}$ coefficients in axisymmetric velocity field representation
a dimensionless parameter determined by the ratio of the gap width to the mean radius of the annulus, $s/2r_m$
$B_{m,n,k}, C_{m,n,k}$ coefficients in asymmetric velocity field representation
$G_{m,n,k}$ coefficients in temperature field representation
$\mathbf{e}_r, \mathbf{e}_\phi, \mathbf{e}_z$ unit vectors in r-, ϕ-, z-directions, respectively
g acceleration of gravity
KF number of vertical trial functions
H height of the annulus
m azimuthal mode number
NF number of radial trial functions
p dimensionless pressure field
Pr Prandtl number, ν/κ
Ra Rayleigh number, $\alpha\beta g H^4/\kappa\nu$
Ra_c critical Rayleigh number
r dimensionless radial coordinate
r_i, r_o dimensionless radii of the inner and outer cylinders scaled by H, respectively
r_m dimensionless mean radius, $(r_i+r_o)/2$
s dimensionless gap width, r_o-r_i
T_0, T_1 temperatures at the bottom and top surfaces
$\mathbf{u}$ dimensionless velocity field, (u_r, u_ϕ, u_z)
x transformed radial coordinate, $r = r_m(1+ax)$
z dimensionless vertical coordinate.

Greek symbols
α coefficients of thermal expansion
β adverse temperature gradient of the initial state in the vertical direction, $(T_0-T_1)/H$
θ dimensionless temperature field
κ thermal diffusivity
λ_k eigenvalue in beam function
ν kinematic viscosity
ρ_0 mean density
ϕ azimuthal coordinate.

Subscript
$*$ dimensional quantity.

Other symbol
∇^2 Laplacian, $\partial^2/\partial r^2+(1/r)(\partial/\partial r)+(1/r^2)(\partial^2/\partial\phi^2)+\partial^2/\partial z^2$.

$$\theta = \frac{1}{\beta H}\theta_*, \quad p = \frac{H^2}{\rho_0\kappa^2}P_*.$$

For convenience, we introduce a new radial coordinate x such that the inner cylinder ($r = r_i$) corresponds to $x = -1$ and the outer ($r = r_o$) to $x = 1$

$$x = \frac{1}{a}\left(\frac{r}{r_m}-1\right); \quad a = \frac{s}{2r_m}. \tag{4}$$

The solutions of equations (1)–(4) are sought for the following boundary conditions:

$$u = 0 \quad \text{on} \quad x = \pm 1\,(-\tfrac{1}{2} \leqslant z \leqslant \tfrac{1}{2}) \quad \text{and on} \quad z = \pm\tfrac{1}{2}(-1 \leqslant x \leqslant 1) \tag{5}$$

$$\theta = 0 \quad \text{on} \quad z = \pm\tfrac{1}{2}(-1 \leqslant x \leqslant 1) \tag{6}$$

$$\theta = 0 \quad \text{on} \quad x = \pm 1\,(-\tfrac{1}{2} \leqslant z \leqslant \tfrac{1}{2}), \quad \text{for perfectly conducting lateral walls} \tag{7}$$

$$\frac{\partial\theta}{\partial x} = 0 \quad \text{on} \quad x = \pm 1\,(-\tfrac{1}{2} \leqslant z \leqslant \tfrac{1}{2}), \quad \text{for perfectly insulating lateral walls.} \tag{8}$$

Equations (1)–(4) with boundary conditions (5), (6) and (7) (or (5), (6) and (8)) constitute an eigenvalue problem for the Rayleigh number Ra. The smallest eigenvalue is the desired critical Rayleigh number.

3. METHOD OF SOLUTION

The Galerkin method is used to solve the eigenvalue problem stated in the previous section. First, the velocity and the temperature fields are represented by a series of trial functions which satisfy the continuity equation (1) and boundary conditions (5)–(7) (or (5), (6) and (8)). Before proceeding, it is useful to point out that the odd solutions in z (corresponding to an even number of vertical rolls) are more stable than the even ones [3, 8] and, therefore, it is sufficient to consider only the temperature and vertical trial functions even in z and the other two velocities odd.

The approximating series for temperature is

$$\theta = \sum_{n=1}^{NF}\sum_{k=1}^{KF} G_{m,n,k}\theta_{m,n,k};$$

$$\theta_{m,n,k} = \cos(m\phi)t_n(x)\cos[(2k-1)\pi z], \quad m = 0, 1, 2, \ldots \tag{9}$$

where m is the mode number (e.g. $m = 0$ is the axisymmetric mode, $m = 1$ the first asymmetric mode, etc.). The radial trial function $t_n(x)$ is chosen to satisfy boundary condition (7) or (8).

(A) Conducting side walls

$$t_n(x) = P_{n+1}(x) - \tfrac{1}{2}[1-(-1)^n]P_0(x) - \tfrac{1}{2}[1+(-1)^n]P_1(x), \quad n = 1, 2, \ldots \tag{10}$$

(B) Insulating side walls

$$t_1(x) = P_0(x)$$

$$t_n(x) = P_{n+1}(x) - \frac{(n+1)(n+2)}{4}[1+(-1)^n]P_1(x) - \frac{(n+1)(n+2)}{12}[1-(-1)^n]P_2(x), \quad n = 2, 3, \ldots \quad (11)$$

where $P_n(x)$ denotes the Legendre polynomial of degree n.

For the approximate representations of the velocity field, it is convenient to treat the axisymmetric mode and the asymmetric (three-dimensional) modes separately. To approximate the axisymmetric velocity field, only one set of stream functions is needed, whereas two two-dimensional velocity fields are necessary to represent the asymmetric velocity fields [3].

(1) Axisymmetric mode

$$\mathbf{u} = \sum_{n=1}^{NF}\sum_{k=1}^{KF} A_{n,k}\mathbf{U}_{n,k}; \quad \mathbf{U}_{n,k} = \operatorname{curl}(\psi_{n,k}\mathbf{e}_\phi), \quad \psi_{n,k}(x,z) = f_n(x)C_k(z) \quad (12)$$

where the radial trial function $f_n(x)$ is chosen as

$$f_n(x) = P_{n+3}(x) + \frac{(n+1)(n+6)}{12}[1-(-1)^n]P_0(x) + \frac{n(n+7)}{20}[1+(-1)^n]P_1(x) - \frac{(n+3)(n+4)}{12}\times[1-(-1)^n]P_2(x) - \frac{(n+2)(n+5)}{20}\times[1+(-1)^n]P_3(x), \quad n = 1, 2, \ldots \quad (13)$$

and the vertical trial function $C_k(z)$ is the even beam function [12]

$$C_k(z) = \frac{\cosh\lambda_k z}{\cosh\lambda_k/2} - \frac{\cos\lambda_k z}{\cos\lambda_k/2} \quad (14)$$

where λ_k satisfies

$$\tanh\frac{\lambda_k}{2} + \tan\frac{\lambda_k}{2} = 0. \quad (15)$$

(2) Asymmetric three-dimensional mode

$$\mathbf{u} = \sum_{n=1}^{NF}\sum_{k=1}^{KF}[B_{m,n,k}\mathbf{V}^{(1)}_{m,n,k} + C_{m,n,k}\mathbf{V}^{(2)}_{m,n,k}]; \quad m = 1, 2, \ldots \quad (16)$$

$$\mathbf{V}^{(1)}_{m,n,k} = \operatorname{curl}(\psi^{(1)}_{m,n,k}\mathbf{e}_r)$$

$$\mathbf{V}^{(2)}_{m,n,k} = \operatorname{curl}(\psi^{(2)}_{m,n,k}\mathbf{e}_z)$$

$$\psi^{(1)}_{m,n,k} = \sin m\phi\, g_n(x)C_k(z)$$

$$\psi^{(2)}_{m,n,k} = \sin m\phi\, f_n(x)\sin 2k\pi z$$

where

$$g_n(x) = \begin{cases} P_{n+1}(x) - 1 & (n = 1, 3, 5, \ldots) \\ P_{n+1}(x) - x & (n = 2, 4, 6, \ldots) \end{cases}$$

and $f_n(x)$ is given by equation (13).

Note that each of $\mathbf{U}_{n,k}$, $\mathbf{V}^{(1)}_{m,n,k}$ and $\mathbf{V}^{(2)}_{m,n,k}$ satisfies the no-slip conditions on the bounding surfaces and that the velocity field given by equation (12) or equation (16) satisfies the continuity equation (1). We have chosen the radial trial functions as linear combinations of Legendre polynomials $P_n(x)$, since a sufficient number of radial functions in this form will give exponentially accurate results [13].

Substituting the expressions for $\mathbf{u}$ and θ in equations (2) and (3) and requiring that the residuals be orthogonal to all the trial functions, a system of linear algebraic equations for the coefficients $A_{n,k}$, $B_{m,n,k}$, $C_{m,n,k}$ and $G_{m,n,k}$ is obtained.

For brevity, only the description for the asymmetric mode will be given below. Equations (2) and (3), together with expressions (9) and (16), yield the following $3N$ ($N = NF^*KF$) linear equations:

$$\begin{bmatrix} [M_{11}] & [M_{12}] & Ra[M_{13}] \\ [M_{21}] & [M_{22}] & 0 \\ [M_{31}] & 0 & [M_{33}] \end{bmatrix}\begin{Bmatrix} \bar{B} \\ \bar{C} \\ \bar{G} \end{Bmatrix} = 0 \quad (17)$$

where $[M_{ij}]$ are $N\times N$ matrices and $\bar{B}$, $\bar{C}$ and $\bar{G}$ are N-dimensional column matrices of $B_{m,n,k}$, $C_{m,n,k}$ and $G_{m,n,k}$, respectively

$$[M_{11}] = \langle(\nabla^2\mathbf{V}^{(1)}_{m,n,k})\cdot\mathbf{V}^{(1)}_{m,p,q}\rangle$$

$$[M_{12}] = \langle(\nabla^2\mathbf{V}^{(2)}_{m,n,k})\cdot\mathbf{V}^{(1)}_{m,p,q}\rangle$$

$$[M_{13}] = \langle(\theta_{m,n,k}\mathbf{e}_z)\cdot\mathbf{V}^{(1)}_{m,p,q}\rangle$$

$$[M_{21}] = \langle(\nabla^2\mathbf{V}^{(1)}_{m,n,k})\cdot\mathbf{V}^{(2)}_{m,p,q}\rangle$$

$$[M_{22}] = \langle(\nabla^2\mathbf{V}^{(2)}_{m,n,k})\cdot\mathbf{V}^{(2)}_{m,p,q}\rangle$$

$$[M_{31}] = \langle(\mathbf{V}^{(1)}_{m,n,k})\cdot(\theta_{m,p,q}\mathbf{e}_z)\rangle$$

$$[M_{33}] = \langle(\nabla^2\theta_{m,n,k})\cdot\theta_{m,p,q}\rangle$$

$$p = 1, \ldots, NF, \quad q = 1, \ldots, KF. \quad (18)$$

Here, the inner product of vector functions $\langle\mathbf{f}\cdot\mathbf{g}\rangle$ is defined as

$$\langle\mathbf{f}\cdot\mathbf{g}\rangle = \int_{-1/2}^{1/2}\int_0^{2\pi}\int_{-1}^{1}(\mathbf{f}\cdot\mathbf{g})(1+ax)\,\mathrm{d}x\,\mathrm{d}\phi\,\mathrm{d}z. \quad (19)$$

The terms involving pressure vanish due to the solenoidal characteristics of the vector field and the boundary conditions.

Elimination of $\bar{C}$ and $\bar{G}$ in equation (17) yields the following N linear equations:

$$([M_{11}] - [M_{12}][M_{22}]^{-1}[M_{21}] - Ra[M_{13}][M_{33}]^{-1}[M_{31}])\bar{B} = 0. \quad (20)$$

The requirement for the system of N linear equations (20) to have non-trivial solution is that the secular determinant be zero

$$\det([M_{11}]-[M_{12}][M_{22}]^{-1}[M_{21}] - Ra[M_{13}][M_{33}]^{-1}[M_{31}]) = 0. \quad (21)$$

Solving this eigenvalue equation for a fixed m, we can find the corresponding Rayleigh number and the resulting flow field. The repeated use of this procedure gives the Rayleigh number for each value of m ($m = 1, 2, \ldots$). The axisymmetric case ($m = 0$) can be solved in a similar manner. The critical Rayleigh number and the corresponding preferred mode are determined by comparing the axisymmetric and asymmetric results for a fixed geometrical configuration. The desired critical mode m is the one that gives the smallest Rayleigh number, i.e. critical Rayleigh number Ra_c.

4. RESULTS AND DISCUSSION

Calculations were carried out for gap width to depth ratio $s \leqslant 3.5$ and gap width to mean radius ratio $2a \leqslant 1.9$. A sufficient number of trial functions were used to give the critical Rayleigh numbers accurate to three significant figures. For all the cases calculated, 24 terms (8 radial and 3 vertical trial functions) insured the desired accuracy.

A two-dimensional channel can be regarded as the limit of an annulus as $a \to 0$ with fixed s. When $a = 0.01$ instead of zero and $s = 1$, we obtained $Ra_c = 5020$ associated with an axisymmetric ring roll and $Ra_c = 3140$ associated with radial rolls (asymmetric rolls with axes directed radially), for conducting lateral walls. Davis [3] reported that for a long rectangular box of square cross-section (long side to height ratio = 10) with conducting bounding walls $Ra_c = 5035$ in association with a single finite roll with axis parallel to the long side and $Ra_c \leqslant 3500$ associated with finite rolls with axes parallel to the short side. The results obtained for the annulus and those for the rectangular box compare favorably, which may provide a check for the present calculations.

In Fig. 2, theoretically predicted critical Rayleigh numbers and preferred modes at the onset of convection are depicted as functions of gap width s for fixed mean radius $r_m = 4$, and are compared with those experimentally observed by Stork and Müller [10]. Both the critical Rayleigh number and the configurations show good agreement between the theoretical calculations for insulated side walls and experimental observations. For small gap width ($s \leqslant 1$), the thermal boundary condition on side walls strongly affects the critical states (critical Rayleigh number and cell modes). It is to be noted that, for conducting side walls, the number of radial rolls rapidly increases as gap width decreases, while it remains unchanged (number of cells = 26) for insulating walls. The variation of roll numbers for small s observed by Stork and Müller [10] may be due to the fact that side walls in the experiment are not perfectly insulating. For large gap width ($s \gtrsim 2$), the critical states are almost independent of thermal conditions on lateral walls and the critical Rayleigh number decreases to 1708, as the gap width increases.

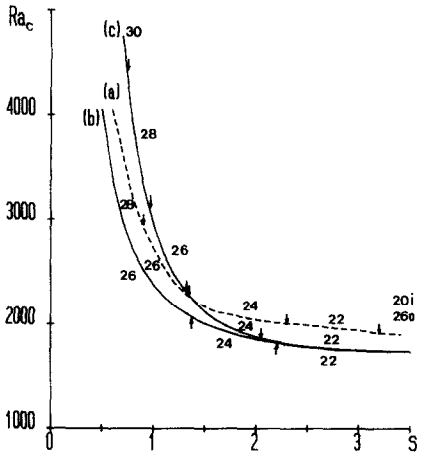

FIG. 2. Critical Rayleigh number Ra_c as a function of gap width s for $r_m = 4$. Curve (a), experimental results by Stork and Müller [10] with insulating side walls. Curves (b) and (c), theoretical results with insulating and conducting side walls, respectively. The numbers indicated near the critical curves denote the number of rolls and the arrows mark the ranges of different roll numbers. The letters 'i' and 'o' indicate the roll numbers experimentally observed at the inner and outer radii, respectively.

Figures 3 and 4 show the critical states for fixed a (fixed outer to inner radius ratio). Figure 3 ($a = 0.95$ or $r_o/r_i = 39$) shows that the presence of an inner cylinder, however small in radius, has significant effects on critical states (see also Figs. 5 and 6). For small s (tall annulus), introduction of an inner cylinder con-

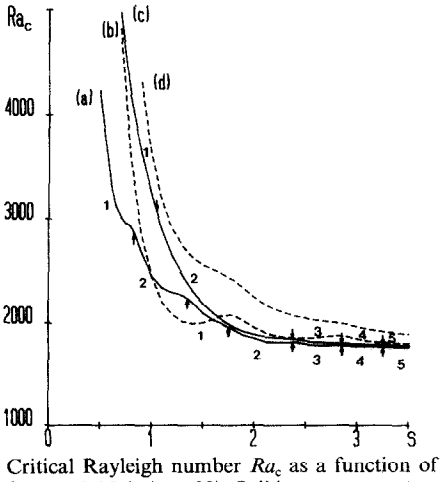

FIG. 3. Critical Rayleigh number Ra_c as a function of gap width s for $a = 0.95$ ($r_o/r_i = 39$). Solid curves correspond to asymmetric modes and dotted curves to the axisymmetric mode. Curves (a) and (b) for insulating lateral walls; curves (c) and (d) for conducting side walls. The numbers indicate the preferred modes (m) and the arrows mark transition points. The figure shows that axisymmetric critical states are possible only for insulating side walls with $1.0 < s < 1.6$.

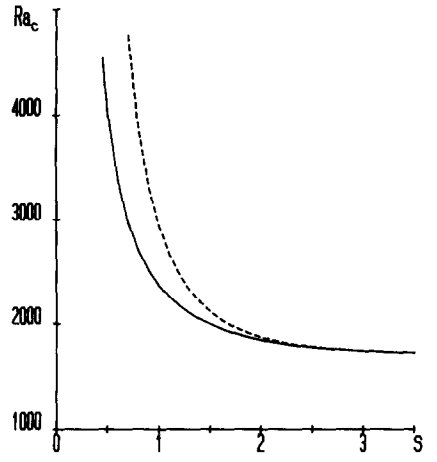

FIG. 4. Critical Rayleigh number Ra_c as a function of gap width for $a = 0.05$ ($r_o/r_i = 1.1$). Solid line corresponds to insulating side walls and dotted line to conducting walls.

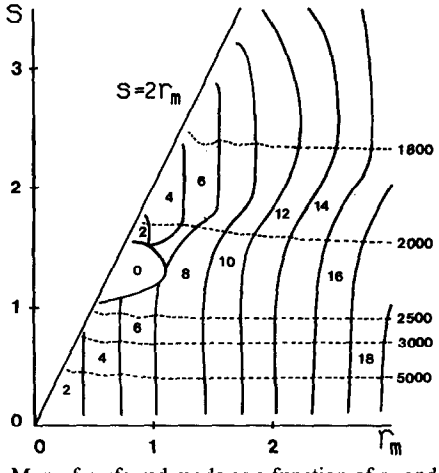

FIG. 5. Map of preferred mode as a function of r_m and s for insulating side walls. Each number indicated represents the number of radial rolls (0 corresponds to the axisymmetric ring roll). Dotted lines are of constant critical Rayleigh number. The boundary $s = 2r_m$ corresponds to $r_i = 0$.

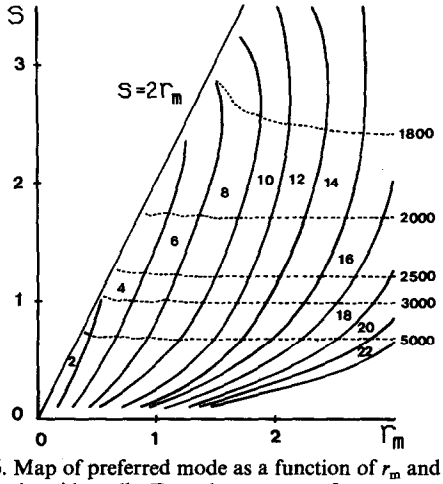

FIG. 6. Map of preferred mode as a function of r_m and s for conducting side walls. Dotted curves are of constant critical Rayleigh number.

siderably raises the critical Rayleigh number Ra_c which is seen to be strongly dependent on the thermal boundary condition on side walls. For large s (fat annulus), the effect of an inner cylinder on the critical Rayleigh number Ra_c diminishes and Ra_c approaches that of the fluid layer confined in a circular cylinder of radius s, although preferred mode configurations are quite different. A notable fact is that the introduction of the inner cylinder has a greater stabilizing effect on axisymmetric disturbances than on asymmetric ones. Figure 4 ($a = 0.05$ or $r_o/r_i = 1.1$) illustrates the critical states of the fluid in an annulus which approximates a long box or a two-dimensional channel. The critical Rayleigh numbers are a little lower than those obtained by Catton [4, 5] for rectangular boxes with conducting or insulating side walls. The result shows that the effect of thermal boundary conditions on side walls diminishes when s is larger than about 2.

Maps of the preferred mode according to linear theory are shown in Figs. 5 (insulating side walls) and 6 (conducting side walls). The numbers appearing in the various zones denote the preferred number of radial rolls contained in the annulus. For small s, preferred modes are radial rolls with only azimuthal and axial velocity components dependent on the three spatial variables, which correspond to finite rolls in a rectangular box [3]. As s increases, the magnitude of the radial velocity component grows appreciably and the velocity field of each radial roll becomes fully three-dimensional. The critical Rayleigh number is mainly determined by the gap width s and little affected by the mean radius r_m; especially when $r_m/s > 1$, Ra_c is nearly independent of r_m (although there are cell transitions).

For insulating side walls, preferred convective modes are mainly determined by r_m. The number of radial rolls is an even integer approximately equal to $2\pi r_m$ for moderately small s, which implies that the roll possesses a square cross-section at the mean radius of the gap. On the other hand, for conducting lateral walls, the number of radial rolls rapidly increases as r_m increases or s decreases when s is small. It is to be noted that introduction of the inner cylinder suppresses the occurrence of the axisymmetric mode. For conducting side walls, the axisymmetric mode does not appear for any combination of gap width and mean radius calculated.

REFERENCES

1. S. Ostrach and D. Pnueli, The thermal instability of completely confined fluids inside some particular configurations, *J. Heat Transfer* **85C**, 346–354 (1963).
2. S. Rosenblat, Thermal convection in a vertical circular cylinder, *J. Fluid Mech.* **122**, 395–410 (1982).
3. S. H. Davis, Convection in a box: linear theory, *J. Fluid Mech.* **30**, 465–478 (1967).
4. I. Catton, Convection in a closed rectangular region: the onset of motion, *J. Heat Transfer* **92C**, 186–188 (1970).

5. I. Catton, The effect of insulating vertical walls on the onset of motion in a fluid heated from below, *Int. J. Heat Mass Transfer* **15,** 665–672 (1972).
6. G. S. Charlson and R. L. Sani, Thermoconvective instability in a bounded cylindrical fluid layer, *Int. J. Heat Mass Transfer* **13,** 1479–1495 (1970).
7. G. S. Charlson and R. L. Sani, On thermoconvective instability in a bounded cylindrical fluid layer, *Int. J. Heat Mass Transfer* **14,** 2157–2160 (1971).
8. J. C. Buell and I. Catton, The effect of wall conduction on the stability of a fluid in a right circular cylinder heated from below, *J. Heat Transfer* **105C,** 255–260 (1983).
9. K. Stork and U. Müller, Convection in boxes: experiments, *J. Fluid Mech.* **54,** 599–611 (1972).
10. K. Stork and U. Müller, Convection in boxes: an experimental investigation in vertical cylinder and annuli, *J. Fluid Mech.* **71,** 231–240 (1975).
11. H. Ozoe, T. Okamoto and S. W. Churchill, Natural convection in a vertical annular space heated from below, *Kagaku Kogaku Ronbunshu* **5,** 457–463 (1979). English translation, *Heat Transfer—Jap. Res.* **8,** 82–93 (1979).
12. S. Chandrasekhar, *Hydrodynamic and Hydromagnetic Instability*. Clarendon Press, Oxford (1961).
13. D. Gottlieb and S. A. Orszag, *Numerical Analysis of Spectral Method: Theory and Applications*, MSF-CBMS Monograph No. 26. Soc. Ind. Appl. Math., Philadelphia (1981).

INSTABILITE DE CONVECTION POUR UNE COUCHE FLUIDE CONFINEE DANS UN ESPACE ANNULAIRE VERTICAL CHAUFFE PAR LE BAS

Résumé—L'apparition de la convection naturelle dans une couche fluide complètement confinée dans un espace annulaire vertical, chauffé par le bas est étudiée sur la base de la théorie linéaire de stabilité. Les nombres de Rayleigh critiques et les configurations des cellules préférentielles sont déterminés en fonction du rayon moyen et de la largeur de l'espace pour une profondeur donnée de la couche. Les résultats sont en bon accord avec les observations expérimentales de Stork et Müller.

KONVEKTIONSINSTABILITÄT EINER VON UNTEN BEHEIZTEN FLÜSSIGKEITSSCHICHT IN EINEM VERTIKALEN RINGKANAL

Zusammenfassung—Es wird das Einsetzen der natürlichen Konvektion in einer von unten beheizten Flüssigkeitsschicht, die vollständig von einem vertikalen Ringkanal begrenzt wird, mit Hilfe der linearen Stabilitätstheorie untersucht. Die kritischen Rayleigh- Zahlen und die bevorzugten Zellenstrukturen werden in Abhängigkeit des mittleren Radius und der Spaltbreite für eine gegebene Schichtdicke bestimmt. Die Ergebnisse zeigen gute Übereinstimmung mit den experimentellen Beobachtungen von Stork und Müller.

КОНВЕКТИВНАЯ НЕУСТОЙЧИВОСТЬ СЛОЯ ЖИДКОСТИ В НАГРЕВАЕМОМ СНИЗУ ВЕРТИКАЛЬНОМ КОЛЬЦЕВОМ КАНАЛЕ

Аннотация—На основе линейной теории устойчивости исследуется возникновение естественной конвекции в нагреваемом снизу слое жидкости в вертикальном кольцевом канале. Критические значения числа Рэлея и предпочтительная форма ячеек определены в зависимости от среднего радиуса и величины зазора для данной высоты слоя. Результаты исследования хорошо согласуются с экспериментальными данными Шторка и Мюллера.